Research Article Vol. 56, No. 18 / June 20 2017 / Applied Optics 5139

applied optics

Zonal wavefront reconstruction in quadrilateral geometry for phase measuring deflectometry

Lei Huang,[1,*] Junpeng Xue,[1,2] Bo Gao,[1,3,4] Chao Zuo,[5] and Mourad Idir[1]

[1]Brookhaven National Laboratory—NSLS II, 50 Rutherford Dr. Upton, New York 11973-5000, USA
[2]School of Aeronautics and Astronautics, Sichuan University, Chengdu 610065, China
[3]Shanghai Institute of Applied Physics, Chinese Academy of Sciences, Shanghai 201800, China
[4]University of Chinese Academy of Sciences, Beijing 100049, China
[5]Jiangsu Key Laboratory of Spectral Imaging & Intelligence Sense, Nanjing University of Science and Technology, Nanjing 210094, China
*Corresponding author: huanglei0114@gmail.com

Received 21 March 2017; revised 8 May 2017; accepted 23 May 2017; posted 24 May 2017 (Doc. ID 290957); published 14 June 2017

There are wide applications for zonal reconstruction methods in slope-based metrology due to its good capability of reconstructing the local details on surface profile. It was noticed in the literature that large reconstruction errors occur when using zonal reconstruction methods designed for rectangular geometry to process slopes in a quadrilateral geometry, which is a more general geometry with phase measuring deflectometry. In this work, we present a new idea for the zonal methods for quadrilateral geometry. Instead of employing the intermediate slopes to set up height-slope equations, we consider the height increment as a more general connector to establish the height-slope relations for least-squares regression. The classical zonal methods and interpolation-assisted zonal methods are compared with our proposal. Results of both simulation and experiment demonstrate the effectiveness of the proposed idea. In implementation, the modification on the classical zonal methods is addressed. The new methods preserve many good aspects of the classical ones, such as the ability to handle a large incomplete slope dataset in an arbitrary aperture, and the low computational complexity comparable with the classical zonal method. Of course, the accuracy of the new methods is much higher when integrating the slopes in quadrilateral geometry.

OCIS codes: (120.0120) Instrumentation, measurement, and metrology; (120.3940) Metrology; (150.6910) Three-dimensional sensing; (120.6650) Surface measurements, figure.

https://doi.org/10.1364/AO.56.005139

1. INTRODUCTION

The two-dimensional shape/wavefront reconstruction is a key process in slope-measuring profiling techniques, such as phase measuring deflectometry such as phase measuring deflectometry (PMD) [1–5], which reconstruct the surface height as a final result from the measured slopes. Many efforts have been made to improve the reconstruction accuracy as well as the integration speed. In the literature, there are two major families in wavefront reconstruction. One large family is named "zonal wavefront reconstruction" [2,6,7], which uses local relations between heights and slopes to connect all the valid measures with unknown height values and finally estimate the height with a least-squares method. The other one is called "modal wavefront reconstruction" [8–10], which describes the surface shape and its slopes with a certain mathematical model, e.g., Zernikes, and uses the measured slopes to estimate the coefficients in the model to represent the height distribution by the mathematical model with the determined coefficients.

Comparing to the modal methods, the zonal methods are good at reconstructing the local detailed features, and therefore they have been widely applied in phase measuring deflectometry, which can measure free-form specular surfaces. The zonal reconstruction is proposed in rectangular geometry [6]. However, the mesh grids in phase measuring deflectometry are generally in quadrilateral geometry, due to its off-axis configuration and lens distortion. Through a comparison work on the existing zonal reconstruction methods [11], it is noticed that directly applying zonal algorithms developed for rectangular geometry to process the slopes in quadrilateral geometry can generate large reconstruction errors and ruin the technique-claimed accuracy as a result. Recently, Ren *et al.* suggested two methods [4,5] to overcome this issue. The first one [4] interpolates x- and y-slope values in a rectangular mesh at first, and then applies the zonal integration for rectangular geometry to get the height distribution on the rectangular mesh, and at last interpolates back to the quadrilateral geometry again if the height in the original geometry is wanted. The other method [5] connects the height and slopes with assistance from another integration method, such as radial basis functions, as a supplementary constraint. In this work, we present a simple,

straightforward, and efficient approach to deal with the zonal wavefront reconstruction in quadrilateral geometry. By considering the height increments between two neighboring grids in the x- and y-directions, this approach can be regarded as a more general form of the zonal wavefront reconstruction.

2. PRINCIPLE OF THE PROPOSED METHOD

In the existing zonal methods [6,7,12], the slope value at the halfway position between two neighboring sampling points is treated as the connector and described by either the unknown heights at sampling locations or the measured slopes locally, and these two expressions should be equal in a least-squares sense as Eq. (1). It is correct and straightforward to implement in a rectangular geometry:

$$\begin{cases} \frac{z_{m,n+1}-z_{m,n}}{x_{m,n+1}-x_{m,n}} \triangleq f_{m,n+\frac{1}{2}}(s^x) \\ \frac{z_{m+1,n}-z_{m,n}}{y_{m+1,n}-y_{m,n}} \triangleq f_{m+\frac{1}{2},n}(s^y) \end{cases}, \tag{1}$$

where $x_{m,n}$, $y_{m,n}$, and $z_{m,n}$ are the coordinates at (m, n). s^x and s^y are the measured x-slope and y-slope. $f_{m,n+\frac{1}{2}}(\cdot)$ and $f_{m+\frac{1}{2},n}(\cdot)$ are local slope functions for the x-direction and y-direction. The expressions of those local slope functions depend on the selected zonal reconstruction method, e.g., $f_{m,n+\frac{1}{2}}(s^x) = (s^x_{m,n} + s^x_{m,n+1})/2$ and $f_{m+\frac{1}{2},n}(s^y) = (s^y_{m,n} + s^y_{m+1,n})/2$ in Southwell's method [6].

However, the locations where slopes are measured may not be in a perfect rectangular geometry in a practical measurement. As illustrated in Fig. 1, several types of sampling position errors can contribute to the final data mesh, e.g., the random positioning error, the lens distortion, and perspective effect, or say keystone. In fact, any of the effects mentioned above will change the ideal rectangles into quadrilaterals in general.

Facing a quadrilateral geometry, the existing zonal methods have difficulty in implementation, more particularly, the creation of the height-slope relations, because the slope value at the halfway position is no longer a pure x-slope or y-slope as it was in a rectangular mesh and the description of this slope with unknown heights at sampling locations cannot separate the contributions from the x- and y-slopes, as shown in Fig. 2(a). As a result, the height-slope relations between the unknown height and the measured slopes cannot be established.

We consider this problem from a different angle, as shown in Fig. 2(b). Instead of linking the unknown heights and measured slopes with an intermediate slope, the height increments are considered as the connectors as Eq. (2):

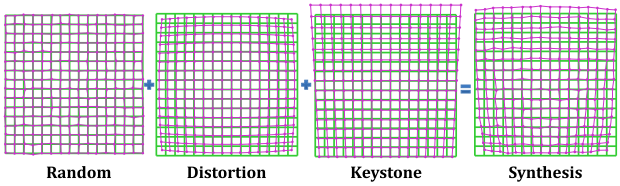

Fig. 1. Several effects in practice can make a rectangular mesh become quadrilateral, and usually these effects work together.

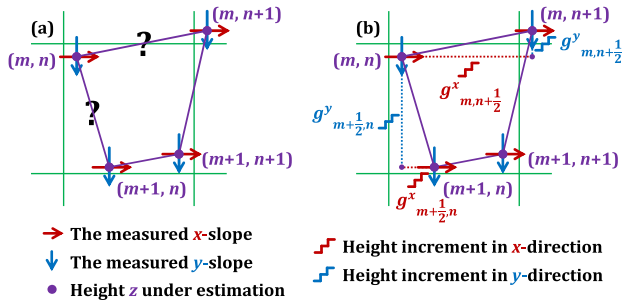

Fig. 2. Height-slope relations are not easy to establish with an "intermediate slope" (a), but they can be established by considering the "height increments" as connectors (b).

$$\begin{cases} z_{m,n+1} - z_{m,n} \triangleq g^x_{m,n+\frac{1}{2}} + g^y_{m,n+\frac{1}{2}} \\ z_{m+1,n} - z_{m,n} \triangleq g^x_{m+\frac{1}{2},n} + g^y_{m+\frac{1}{2},n} \end{cases}, \tag{2}$$

where the height increments at different sections described by the x-slopes and y-slopes are

$$g^x_{m,n+\frac{1}{2}} = f_{m,n+\frac{1}{2}}(s^x)(x_{m,n+1} - x_{m,n}), \tag{3}$$

$$g^y_{m,n+\frac{1}{2}} = f_{m,n+\frac{1}{2}}(s^y)(y_{m,n+1} - y_{m,n}), \tag{4}$$

$$g^x_{m+\frac{1}{2},n} = f_{m+\frac{1}{2},n}(s^x)(x_{m+1,n} - x_{m,n}), \tag{5}$$

$$g^y_{m+\frac{1}{2},n} = f_{m+\frac{1}{2},n}(s^y)(y_{m+1,n} - y_{m,n}). \tag{6}$$

In this way, the contributions from the x-slopes and y-slopes can be successfully separated, which is essential to build the connections from the unknown heights with the measured slopes. Equations (2)–(6) can be considered as an extension of Eq. (1) and it pushes the zonal reconstruction method from a rectangular geometry to a more general quadrilateral geometry. In the next section, we will show the significance of getting this general solution via simulation.

3. SIMULATION OF RECONSTRUCTION IN QUADRILATERAL GEOMETRY

In our simulation, the height distribution of the surface under test (SUT) is expressed as

$$\begin{aligned} z(x,y) = \Big\{ & 3(1-x)^2 \exp[-x^2 - (y+1)^2]\sqrt{2} \\ & - 10\left(\frac{x}{5} - x^3 - y^5\right)\exp(-x^2 - y^2) \\ & - \frac{1}{3}\exp[-(x+1)^2 - y^2] \Big\} \times 0.1. \end{aligned} \tag{7}$$

Three effects (random error, distortion, and keystone) are simulated to generate a quadrilateral geometry. The random position errors are normally distributed, distortion is simulated by introducing the radial lens distortion, and the keystone phenomenon is generated by setting a certain off-axis viewing angle to the SUT. More implement details can be found in our MATLAB codes [13]. The analytical solutions of the x-slope and y-slope are derived to calculate the corresponding nominal

height values, x- and y-slopes in quadrilateral geometry, as shown in Fig. 3.

Three existing zonal methods for rectangular geometry (ZM-r) [6,7,12] are implemented to demonstrate their large errors when handling data in quadrilateral geometry. The classical Southwell's method [6] is marked as TFLI (traditional finite-difference-based least-squares integration), The Li's method [7] is marked as HFLI (higher-order finite-difference-based least-squares integration), and the recently proposed spline-based integration method [12] is marked as SLI (spline-based least-square integration). The reconstruction error of TFLI, HFLI, and SLI are shown in Figs. 4(a)–4(c), respectively. All error maps are similar, which indicates that the error due to the quadrilateral geometry is dominating the reconstruction error.

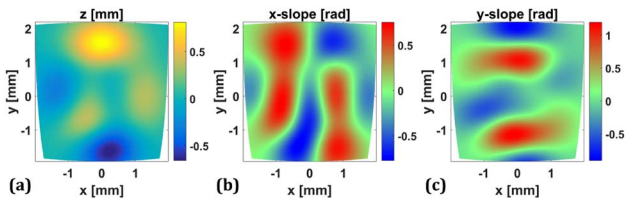

Fig. 3. (a) Analytical height, (b) x-slope, and (c) y-slope in quadrilateral geometry are simulated as the nominal values.

By using the interpolation-assisted strategy proposed in [4], the x- and y-slopes can be interpolated into a rectangular geometry first, and then use the zonal methods to integrate the new slopes to get a height map in the pre-defined rectangular geometry. Lastly, the final height in the original quadrilateral geometry is calculated via another interpolation. These interpolation-assisted zonal methods (ZM-i) are able to handle the slopes in quadrilateral geometry, and they are marked as TFLIi, HFLIi, and SLIi in our comparison. The letter "i" stands for the interpolation version. Their reconstruction error maps are shown in Fig. 4(d) for TFLIi, Fig. 4(e) for HFLIi, and Fig. 4(f) for SLIi. The reconstruction error is smaller, and noticeable error is found at the boundary areas due to the interpolation operation. Increasing the sampling numbers during the slope interpolation may reduce the resultant error at the boundary regions, but the drawback is it will take obviously longer time to complete the interpolation and integration.

With the proposed "height increments" strategy in this work, these existing zonal methods can be modified to be new zonal methods applicable for quadrilateral geometry (ZM-q) and marked as TFLIq, HFLIq, and SLIq, accordingly. The letter "q" stands for the quadrilateral version. Their reconstruction error maps are shown in Fig. 4(g) for TFLIq, Fig. 4(h) for HFLIq, and Fig. 4(i) for SLIq. The modified methods highly reduced the reconstruction errors and this simple idea works well for all three zonal methods in use here, which indicates

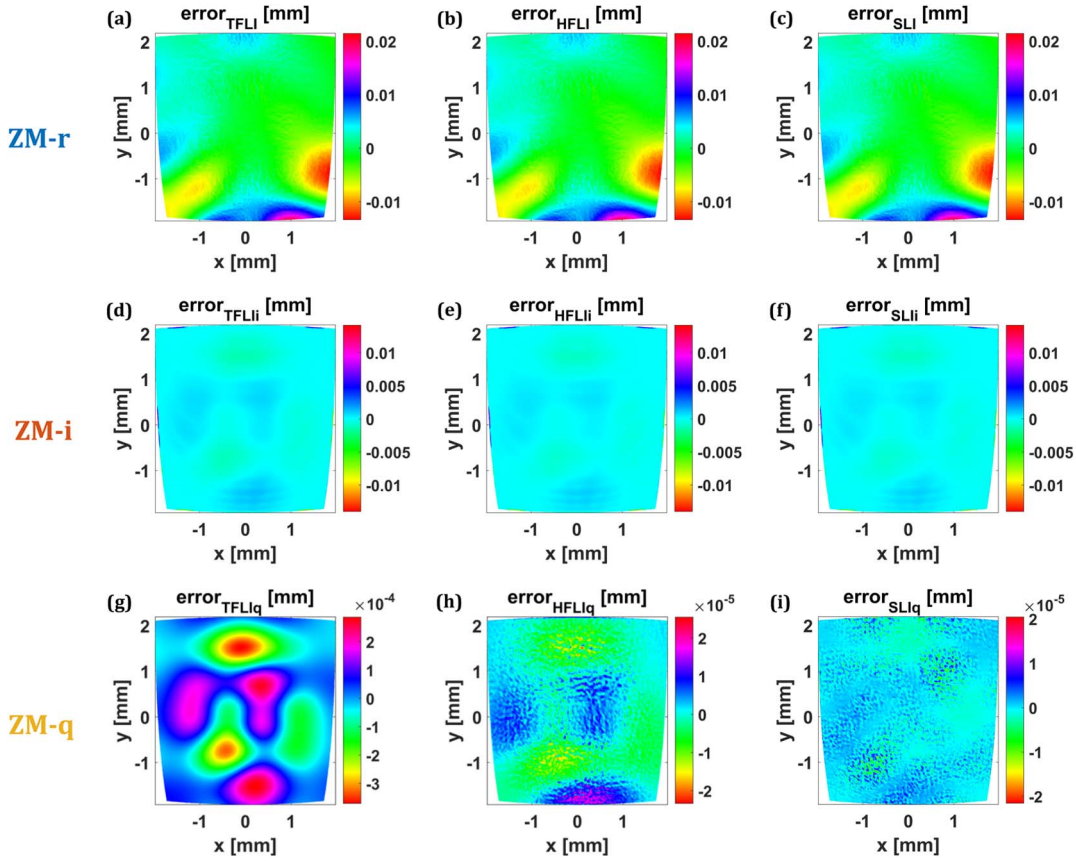

Fig. 4. Existing zonal methods for rectangular geometry generate large reconstruction errors in quadrilateral geometry (a)–(c), while the existing interpolation-assisted zonal methods can improve the performance (d)–(f), and by contrast, the proposed general solutions perform better with far fewer errors (g)–(i).

the new proposal approach pushes the zonal method from rectangular geometry to a more general situation, the quadrilateral geometry. The codes in MATLAB can be downloaded via [13]. This is important for many applications which have quadrilateral data mesh. Next, we will show an experimental case in phase measuring deflectometry.

4. EXPERIMENT

A phase measuring deflectometry setup is used to measure a smooth specular surface, whose size is about 60 mm × 50 mm. The mono-PMD system is composed with a CCD camera (Manta G-145 with 1388 × 1038 pixels and 12-bit pixel depth) and an LCD screen (Dell P2414H with 1920 × 1080 pixels and 0.2745 mm × 0.2745 mm pixel pitch). The system geometry after PMD calibration [14,15] is illustrated in Fig. 5. The camera is about 2.5 m away from the SUT.

The typical fringe patterns from the camera side are shown in Figs. 6(a) and 6(b). The surface slopes and height can be simultaneously determined with a technique called modal phase measuring deflectometry (MPMD) [16,17]. We choose the cubic B-splines with 15 by 15 breaks as the surface model to represent the SUT. The x-slope and y-slope from MPMD in Figs. 6(c) and 6(d) are used as the inputs to test the zonal reconstruction algorithms.

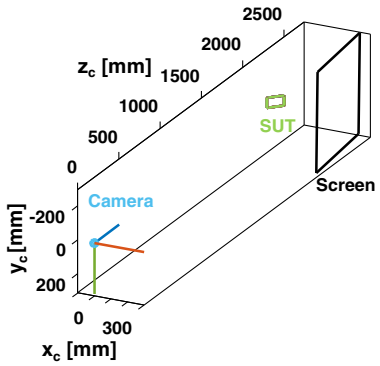

Fig. 5. Calibrated system geometry of phase measuring deflectometry in experiment.

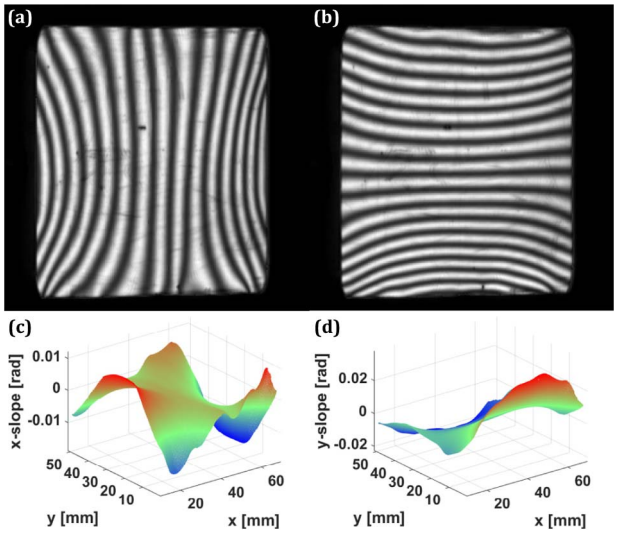

Fig. 6. Typical patterns of (a) x-fringe and (b) y-fringe in the experiment, and the (c) x-slope and (d) y-slope from MPMD.

Because the modal wavefront reconstruction methods use models to represent the slopes and height and these models can be established in any irregular meshes including quadrilateral geometry, intrinsically they can handle slopes in quadrilateral geometry. The idea of modal wavefront reconstruction is inherently used inside the iterations of MPMD; therefore, the resultant height from MPMD in Fig. 7(a) is treated as our benchmark to make a quantitative evaluation. A good zonal method in quadrilateral geometry should have a good consistency with the benchmark when the same modal-method-delivered slopes are used, especially when there are almost no high-frequency components as the surface in our experiment. For simplicity, we only show the comparison between the HFLI method and the HFLIq method, since the observations are similar for the other groups. The reconstruction results are shown in Fig. 7(b) for HFLI, Fig. 7(d) for HFLIi, and Fig. 7(f) for HFLIq. These three reconstructed results [Figs. 7(b), 7(d), and 7(f)] are close to the modal results [Fig. 7(a)]. Here, the reconstruction error is defined as the discrepancy from the MPMD height result.

Although the distortion and keystone effects are not very evident in our experiment owing to the large camera-to-SUT distance, which is about 2.5 m, it is still obvious that the HFLI method gets much larger reconstruction error in Fig. 7(c) than the HFLIi and HFLIq methods do in Figs. 7(e) and 7(g). Due to the boundary effect of the interpolation in HFLIi, attention is required while interpolating around the edges, otherwise obvious errors may appear in the final height values. The integration result by using the proposed HFLIq method shows good agreement with the MPMD result. Moreover, very similar phenomena are observed when using the TFLIq method and the SLIq method, which indicates that the proposed approach works well in pushing the zonal method from rectangular geometry to quadrilateral geometry.

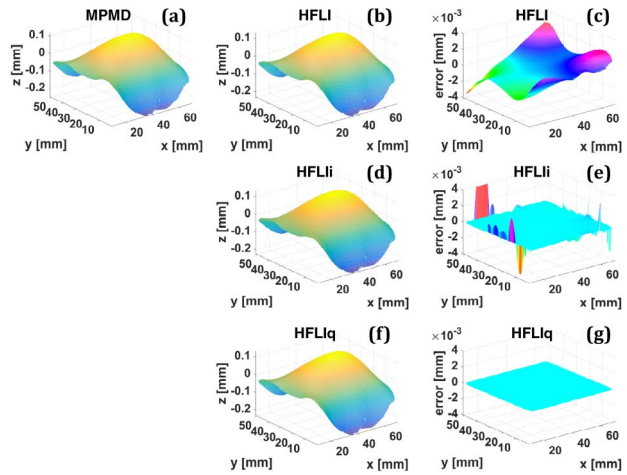

Fig. 7. MPMD reconstructed height (a) is chosen as the benchmark in the evaluation of the zonal reconstruction results of HFLI (b), HFLIi (d), and HFLIq methods (f). The error of HFLI (c) is larger than the error of HFLIi (e) and HFLIq (g).

5. DISCUSSION

The reconstruction accuracy of the proposed ZM-q methods is higher than the existing ZM-r and ZM-i methods when dealing with slopes in quadrilateral geometry. As presented in Fig. 8, the root mean square error (RMSE) of the reconstruction results in Fig. 4 by using different methods indicates the effectiveness of the proposal.

In order to study the noise influence to the proposed methods, the performances with measurement noise on slope are also investigated under the same simulation condition in Section 3. Normally distributed random noises with standard deviation varying from 0 to 20 mrad with a step of 1 mrad are added onto the analytical slopes. The RMSE of the reconstructions by using these nine methods in comparison are shown in Fig. 9.

The RMSEs of reconstruction with the proposed ZM-q (TFLIq, HFLIq, and SLIq) gradually raise up with the increasing of the slope noise, but they are still much lower than those of the methods for rectangular geometry ZM-r (TFLI, HFLI, and SLI) and smaller than those of the interpolation-assisted methods ZM-i (TFLIi, HFLIi, and SLIi) when the error due to sampling geometry is still dominating the reconstruction error.

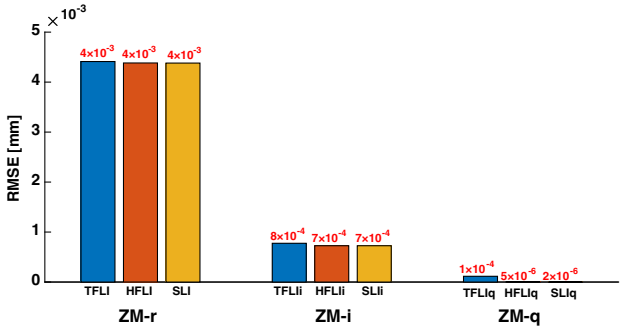

Fig. 8. Proposed methods (ZM-q: TFLIq, HFLIq, SLIq) greatly reduce reconstruction errors when handling slopes in quadrilateral geometry.

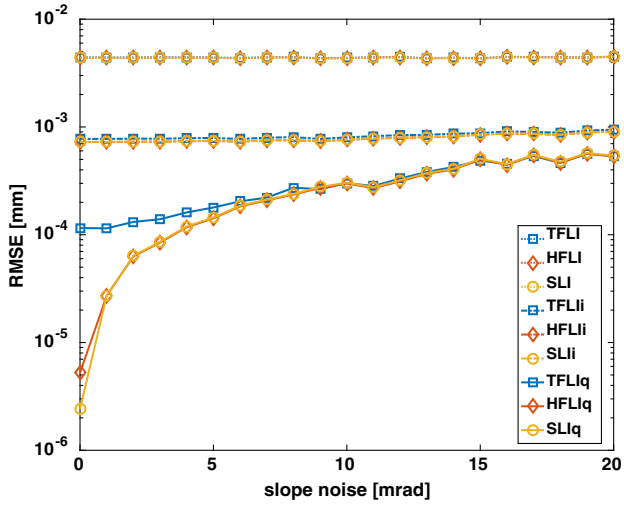

Fig. 9. Reconstruction RMSE of each zonal method changes with the standard deviation of slope noise.

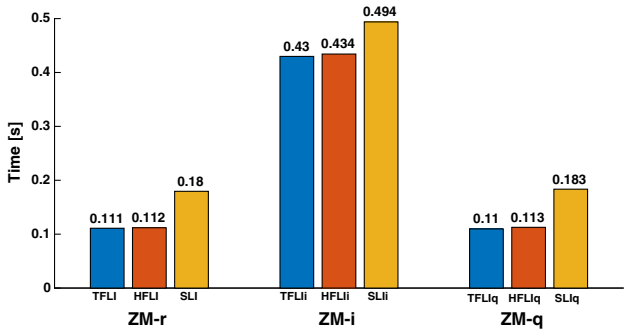

Fig. 10. Speed of the proposed methods ZM-q (TFLIq, HFLIq, SLIq) is close to those methods for rectangular mesh ZM-r (TFLI, HFLI, SLI), and they are faster than the interpolation-assisted versions ZM-i (TFLIi, HFLIi, SLIi), respectively.

In addition, when handling slopes in rectangular geometry, the proposed ZM-q methods are as good as the ZM-r. The height increments in Eqs. (4) and (5) vanish in a rectangular mesh, because $y_{m,n+1} - y_{m,n} = 0$ and $x_{m+1,n} - x_{m,n} = 0$. In this situation, the proposed ZM-q degenerates to its corresponding ZM-r.

The proposed ZM-q (TFLIq, HFLIq, and SLIq) keeps the same sparse matrix as the ZM-r does. It has relatively low memory cost and consequently is good for processing large slope data. Since the major computing time is spent by the inverse operation of that sparse matrix and the additional calculation for height increment in the other direction is negligible, the integration speed of ZM-q is preserved. Therefore the computing time of ZM-q is comparable with ZM-r, as shown in Fig. 10. Owing to the additional time for interpolation, the interpolation-assisted zonal methods ZM-i (TFLIi, HFLIi, and SLIi) are slower than the classical ZM-r and our ZM-q. The speed comparison is carried out with slope datasets with 128×128×2 pixels in MATLAB running on an i7-4600M CPU at 2.90 GHz with 16 GB memory.

In practice, the height increments $g^y_{m,n+\frac{1}{2}}$ in Eq. (4) or $g^x_{m+\frac{1}{2},n}$ in Eq. (5) may not be easy to calculate for the SLIq method, because the splines require the monotonic y to get sectional $f_{m,n+\frac{1}{2}}(s^y)$ or monotonic x to get sectional $f_{m+\frac{1}{2},n}(s^x)$. For convenience, the corresponding height increments $g^y_{m,n+\frac{1}{2}}$ and $g^x_{m+\frac{1}{2},n}$ calculated in the HFLIq method can be used as a simple and accurate substitute.

6. SUMMARY

The zonal wavefront reconstruction in quadrilateral geometry is studied in our work. A new consideration on the height-slope relations is carried out by taking the height increments as connectors instead of using the intermediate slopes in the existing methods. From this new angle, the proposed methods can be established via simple modifications from the existing zonal methods for rectangular geometry, and as a result, the improvements are tremendous. The codes in MATLAB can be

downloaded from [13]. Simulation and experiment are carried out to show the significance in applications with shape reconstruction from slopes in quadrilateral geometry, such as phase measuring deflectometry.

Funding. U.S. Department of Energy (DOE); Office of Science (SC) (DE-SC0012704).

Acknowledgment. This research used resources of the National Synchrotron Light Source II, a U.S. Department of Energy (DOE) Office of Science User Facility operated for the DOE Office of Science by Brookhaven National Laboratory under Contract No. DE-SC0012704.

REFERENCES

1. S. Ettl, J. Kaminski, M. C. Knauer, and G. Häusler, "Shape reconstruction from gradient data," Appl. Opt. **47**, 2091–2097 (2008).
2. L. Huang and A. Asundi, "Improvement of least-squares integration method with iterative compensations in fringe reflectometry," Appl. Opt. **51**, 7459–7465 (2012).
3. L. Huang and A. K. Asundi, "Framework for gradient integration by combining radial basis functions method and least-squares method," Appl. Opt. **52**, 6016–6021 (2013).
4. H. Ren, F. Gao, and X. Jiang, "Improvement of high-order least-squares integration method for stereo deflectometry," Appl. Opt. **54**, 10249–10255 (2015).
5. H. Ren, F. Gao, and X. Jiang, "Least-squares method for data reconstruction from gradient data in deflectometry," Appl. Opt. **55**, 6052–6059 (2016).
6. W. H. Southwell, "Wave-front estimation from wave-front slope measurements," J. Opt. Soc. Am. **70**, 998–1006 (1980).
7. G. Li, Y. Li, K. Liu, X. Ma, and H. Wang, "Improving wavefront reconstruction accuracy by using integration equations with higher-order truncation errors in the Southwell geometry," J. Opt. Soc. Am. A **30**, 1448–1459 (2013).
8. I. Mochi and K. A. Goldberg, "Modal wavefront reconstruction from its gradient," Appl. Opt. **54**, 3780–3785 (2015).
9. M. Ares and S. Royo, "Comparison of cubic B-spline and Zernike-fitting techniques in complex wavefront reconstruction," Appl. Opt. **45**, 6954–6964 (2006).
10. F. Dai, F. Tang, X. Wang, O. Sasaki, and P. Feng, "Modal wavefront reconstruction based on Zernike polynomials for lateral shearing interferometry: comparisons of existing algorithms," Appl. Opt. **51**, 5028–5037 (2012).
11. L. Huang, M. Idir, C. Zuo, K. Kaznatcheev, L. Zhou, and A. Asundi, "Comparison of two-dimensional integration methods for shape reconstruction from gradient data," Opt. Laser Eng. **64**, 1–11 (2015).
12. L. Huang, J. Xue, B. Gao, C. Zuo, and M. Idir, "Spline based least squares integration for two-dimensional shape or wavefront reconstruction," Opt. Laser Eng. **91**, 221–226 (2017).
13. L. Huang, "MATLAB codes for zonal wavefront reconstruction in quadrilateral geometry," https://github.com/huanglei0114/Zonal-wavefront-reconstruction-in-quadrilateral-geometry.
14. Y.-L. Xiao, X. Su, and W. Chen, "Flexible geometrical calibration for fringe-reflection 3D measurement," Opt. Lett. **37**, 620–622 (2012).
15. H. Ren, F. Gao, and X. Jiang, "Iterative optimization calibration method for stereo deflectometry," Opt. Express **23**, 22060–22068 (2015).
16. L. Huang, J. Xue, B. Gao, C. McPherson, J. Beverage, and M. Idir, "Modal phase measuring deflectometry," Opt. Express **24**, 24649–24664 (2016).
17. L. Huang, J. Xue, B. Gao, C. McPherson, J. Beverage, and M. Idir, "Model mismatch analysis and compensation for modal phase measuring deflectometry," Opt. Express **25**, 881–887 (2017).